

Received: 11 January 2019 / Accepted: 18 February 2019 / Published online: 11 March 2019

*additive manufacturing, FLM- simulation,
shape accuracy*

H.-Christian MÖHRING¹
Thomas STEHLE¹
Clemens MAUCHER¹
Dina BECKER^{1*}
Steffen BRAUN¹

PREDICTION OF THE SHAPE ACCURACY OF PARTS FABRICATED BY MEANS OF FLM PROCESS USING FEM SIMULATIONS

The prediction of component properties from the Additive manufacturing (AM) process poses a challenge. Therefore, this paper presents the development of a novel machine data (G-Code) based procedure as well as its programming implementation of a process simulation in ANSYS Mechanical for the fused layer modelling (FLM) process. For this purpose, an investigation of additively produced components with varying parameters made of polylactic acid (PLA) is carried out and simulated by means of the developed method. Application of the developed method makes it possible to predict the thermally induced distortion of PLA-Parts based on the machine data from the FLM process before production.

1. INTRODUCTION

Additive manufacturing (AM) processes allow complex shapes to be created and thus allow to rethink design approaches and optimize existing machine elements [1–5]. AM describes production processes in which solid components are produced by layered construction from a wide variety of shapeless starting materials. Therefore, no moulds or tools are required [6, 7]. The technologies of additive manufacturing itself have matured significantly and offer opportunities to produce products that are not feasible or cost-effective with conventional methods such as machining or injection moulding [3]. Due to this increasing technical maturity of additive manufacturing processes and the associated improvement in product properties, additive manufacturing processes are becoming increasingly important for industrial applications [6, 8]. Thus, the requirements for additively manufactured components increase. For example, in the production of near-net shape components, it is a major challenge to minimize the reworking effort while at

¹ Institute for Machine Tools (IfW), University of Stuttgart, Stuttgart, Germany

* E-mail: dina.becker@ifw.uni-stuttgart.de

<https://doi.org/10.5604/01.3001.0013.0463>

the same time improving component properties [3]. The specification and verification of geometrical tolerances leads to new requirements in design and quality engineering [9–11]. A variety of process parameters, such as material deposition speed and temperature, arrangement and direction of build-up paths, orientation of the part within the workspace of the AM machine, as well as boundary conditions, influences the accuracy and physical properties of the manufactured parts [12, 13]. Consequently, there is a superordinate need to be able to simulate the process of manufacture, as well as to minimize the frequency of possible process-related failures. The most widely used additive process in the field of plastic application is the "fused layer modeling" (FLM) [7]. In this process, simplified, molten plastic is applied to a build platform. The extruder is a heated nozzle. A typical Build-up of an FLM machine is shown in Fig. 1.

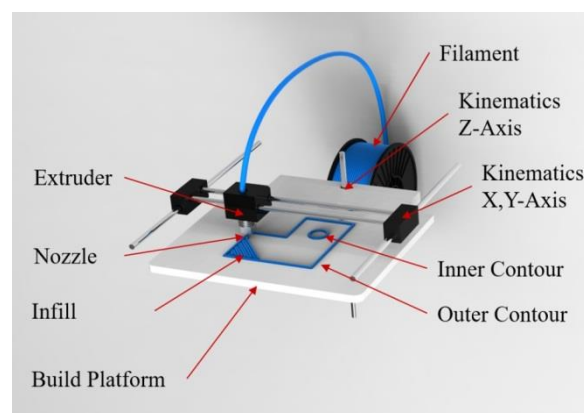


Fig. 1. Build-up of an FLM machine

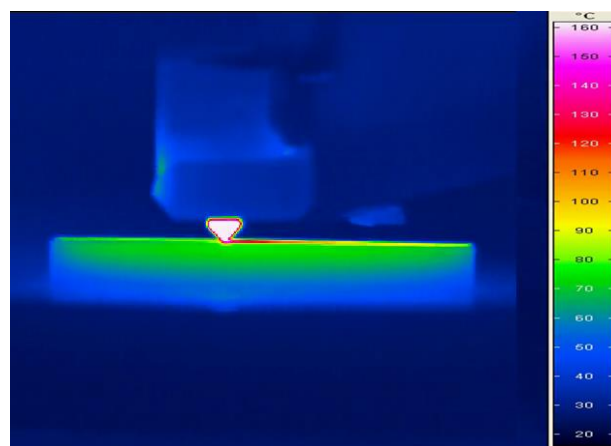


Fig. 2. Thermograph of the printing process

The plastic filaments, which are used to print, are pressed into the extruder by means of a mechanical drive (feeder) and heated with electric heating to just above the melting temperature. This liquid plastic is applied to the previous layer or build platform by the extruder according to the layers of 3D geometry. The liquid plastic strikes the respective

preceding layer (or the build plate) and melts them slightly, cools on contact due to the heat conduction and solidifies. Once the material cools, it hardens quickly. This behaviour was observed by means of a thermography camera. A qualitatively example of the cooling during the process can be seen in Fig. 2. A connection between the still hot plastic layer and the lower, already completed layer takes place only when the material is applied with pressure on the solidified structure. As a result, the still circular section of the applied material in the nozzle is pressed into a rounded rectangle [8].

The cohesion between the pressure-applied path of polymer arises due to the material connection during the cooling process. Since these paths are deposited on each other, the surface quality of the components is usually relatively low [14]. The distance between the preceding layer and the extruder head, as well as the volume flow of the liquid material, are matched to one another in such a way that track widths result as uniform as possible [14].

The advantages of the FLM process include the speed of the printing process, a low production price, the large selection of materials (filaments) with almost complete use of materials and finally the ability to produce compact components with surfaces filled with material. One of the major disadvantages of the method is the limited form accuracy and often required support structures. Therefore, the arrangement or alignment of the parts in the assembly chamber as well as the print kinematics and geometrical parameters of the process has a great influence on their properties and their appearance (shape) [2, 6, 15, 16].

The requirement for additive manufacturing processes to produce a real component from almost any CAD geometry, repeatable and in top quality, is one of the current challenges for companies using additive manufacturing. The use of simulation software, in which printing processes are realistically modelled, is an important solution for optimizing additive manufacturing processes and making them more efficient and cost-effective [17]. Hence, there is a need to simulate the process of additive manufacturing in order to predict various aspects of the process as well as component quality and productivity or ultimately to design the process. The efforts are largely still in the development stage, with some finite element method (FEM) software manufacturers having started to present solutions with a special focus on the metal sector (e.g. for the Selective Laser Melting (SLM) process) [18–25]. Those approaches are using the assumption of “superlayers” which combine multiple layers for the simulation to reduce calculation effort [17]. Those layers are activated successively to simulate the process. However, for this layer-wise approach, there are some restrictions. A limitation of the layer wise approach is that an entire layer is activated at a single time step and, for example, a multiple wall thickness cannot be represented. Another limitation of the stratified calculation is that individual layers are quasi homogenized by the assumption of a preferred direction. No real machine data is used to model the trajectories of the build.

It is also striking that significantly more solutions exist for the metal-based than for the plastic-based processes [18–25]. With increasing economic interest of users of plastic components [26, 27], especially in the field of reinforced plastics, such as PEEK [28], the need to make the FLM process more stable, and to predict the component properties increases. In addition, it is necessary to avoid any failures or inadequate results when using high-quality reinforced plastics, often for several hours of production.

In the study presented here, a method was developed that maps the thermal distortion (warpage) of the FLM process and thus predicts the final shape of the examined components. Accordingly, the shape required during the printing process can then be determined with which the desired geometric final state is achieved after cooling and thermal distortion.

2. EXPERIMENTAL INVESTIGATION

To evaluate the results from the developed simulation method specimen were manufactured to compare the thermal deformation (distortion) which result of the FLM process itself. The specimen, as well as the simulated models were examined for dimensional accuracy. A comparison of the thermal history could not be observed during the manufacturing process.

2.1. TEST COMPONENTS AND MEASUREMENT METHODS

The test specimens were designed in accordance with the guidelines of the standard for determining the tensile properties of plastics DIN EN ISO 527-2 [29] and can be seen in Fig. 3. The focus of the investigations was the flatness on the upper side of the test samples which is marked in Fig. 3. This geometry appeared suitable because it has different cross-sections with uniform areas. In order to investigate the influence and the evenness around boreholes, a hole with a diameter of 5 mm was also inserted. The test sample was designed with the CAD system “ANSYS SpaceClaim” and then exported as STL file, with a maximum deviation of 0.4 mm and a maximum angle error of 4 degrees as tessellation settings.

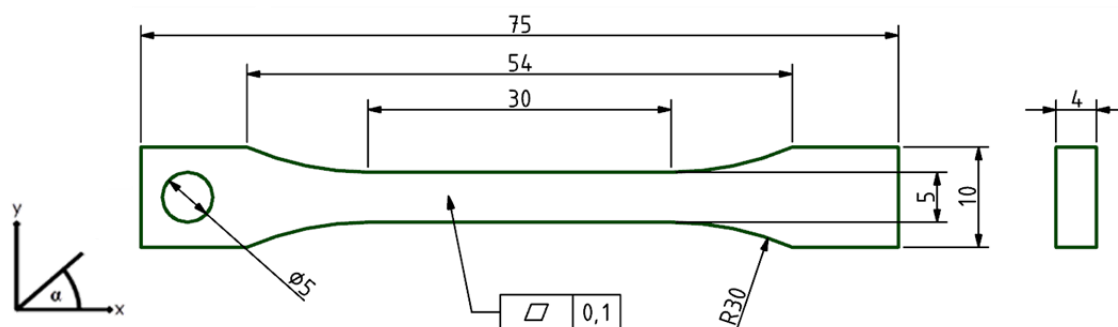


Fig. 3. Geometry of the specimen

The printing material used was the synthetic polymer PLA. PLA is biodegradable and has the potential to replace conventional petrochemical polymers for both industrial and medical applications [30, 31]. The PLA material data important for the FEM were taken

from the preparatory work [32] and literature [33-36]. The dimensional accuracy of the specimens was evaluated using a 3-coordinate measuring machine of the type MC850 from Carl Zeiss AG using an Ultra High Precision Caliper UHPC stylus system (measuring ball radius $R = 2.5$ mm).

2.2. PRODUCTION OF THE TEST SAMPLES IN THE FLM PROCESS

The specimens were manufactured on the 3D printer type Replicator Gen5 manufactured by MakerBot. For all test samples produced, filament by MakerBot of the same spool was used to avoid any variations in material quality. In order to avoid unintended and disturbing air flows from the outside, the side walls of the 3D printer were insulated with polystyrene panels. The acrylic glass build platform was equipped with "Blue Masking Tape" to improve adhesion between the build platform and the part.

The CAD data of the test samples were prepared with the software Simplify3D for the printing process. In this investigation a set of multiple parameters has been examined (Table 1). The slicing settings were adjusted according to the selected parameters. These parameters were chosen because of their great influence on the dimensional accuracy and deformation. However, the printing speed was not considered although its big influence on the shape accuracy to initially test the developed simulation method. The samples were each prepared individually and placed in the same position on the build plate. The specimen manufacturing occurred at room temperature of 22–23°C and the separation from the build plate after a cooling time of 10 min. Five samples were prepared per parameter set, stored for at least 24 h and then measured.

Table 1. Slicer Software Settings

| Setting | Value |
|-----------------------------|--------------|
| Printing speed | 45 mm/s |
| Infill rate | 100 % |
| Infill orientation α | 0°; 45°; 90° |
| Number of contours | 1; 3 |

2.3. FORM ACCURACY OF THE FLM PRINTED SPECIMEN

The test samples were examined on the 3-coordinate measuring machine and evaluated with the help of the programs Calypso (Zeiss AG) and GOM Inspect.

Similar to the preliminary investigations [37–39], it was found that significant differences occur depending on the print direction in the FLM process [32]. Different temperature fields caused by varying webs according to the print direction lead to inhomogeneous volumetric deformations. This effect was found in all samples, especially at the corners, as well as at the edge of the hole in the sample [32]. In part, this can be

attributed to the kinematics of the FLM system or the path planning of the slicer software. Since the paths of the plastic have a start or end point, slight overlaps occur at certain points, which leads to an accumulation of material and thus to a bulge. Furthermore, the extrusion rate of the plastic is kept constant over several webs. In the case of different webs, this leads to a non-uniform material application due to the acceleration (or vibration) of the drive. All test series have in common a large deformation at the edge around the hole.

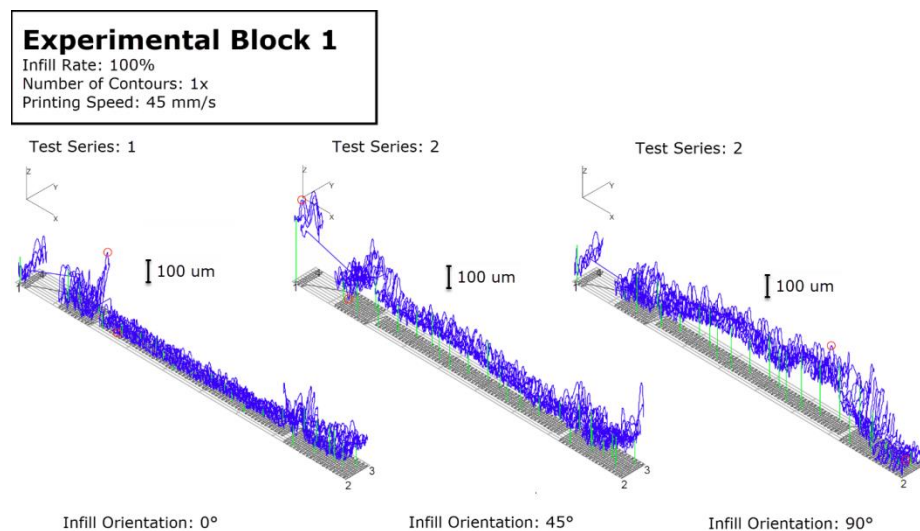


Fig. 4. Typical distribution of the measuring points on the upper printing layer of the specimens (measurement: 3-coordinate measuring machine of the type MC850, manufactured by Carl Zeiss AG)

In the presented study, test samples from the first experimental block were examined for shape accuracy. The test samples were made with 100% fill, a simple wall thickness, with a travel speed of 45 mm/s and with a varying alignment of the filling structure. The results of the survey are shown in Fig. 4. When aligning the fill structure by 0 degrees to the X-axis, there is a slight bulge around the sample waist, but this increases towards the ends of the sample. More uneven are the results for the samples with a 45 degrees orientation. These have a more pronounced bulge, which can be seen particularly strong in the bore. With 90 degrees alignment with the X-axis, a bulge in the area of the sample waist arises upwards. Especially the comparison to the sample with a 0 degrees orientation shows an opposite behaviour of the deformation.

3. SIMULATION OF THE FLM-PROCESS

3.1. GENERAL APPROACH

In order to predict the possible deformations of the FLM process, the production of the specimen was mapped using a transient thermal and a sequential structural numerical simulation with the Software packages of ANSYS. A thermo-mechanical analysis is

required for the calculation of a thermally induced internal stress and the associated distortion in components manufactured in the FLM process [40]. The temperature field calculation is carried out in the first step. In the second step, these time-dependent temperature fields are used as thermal boundary conditions for the mechanical analysis [40].

To simulate the FLM process of the successive material application in a FEM software it took some preliminary work, as this was not possible to represent with standard methods in ANSYS. For the FE calculations, a method was designed, implemented and tested. Unlike the one layer at a time, the method in this paper uses a path-wise approach. The layer wise approach has been investigated for metal based AM process by Keller [17]. The procedure presented here, for calculating the entire process, is shown in Fig. 5. Therein the difference between the two approaches is marked in colour.

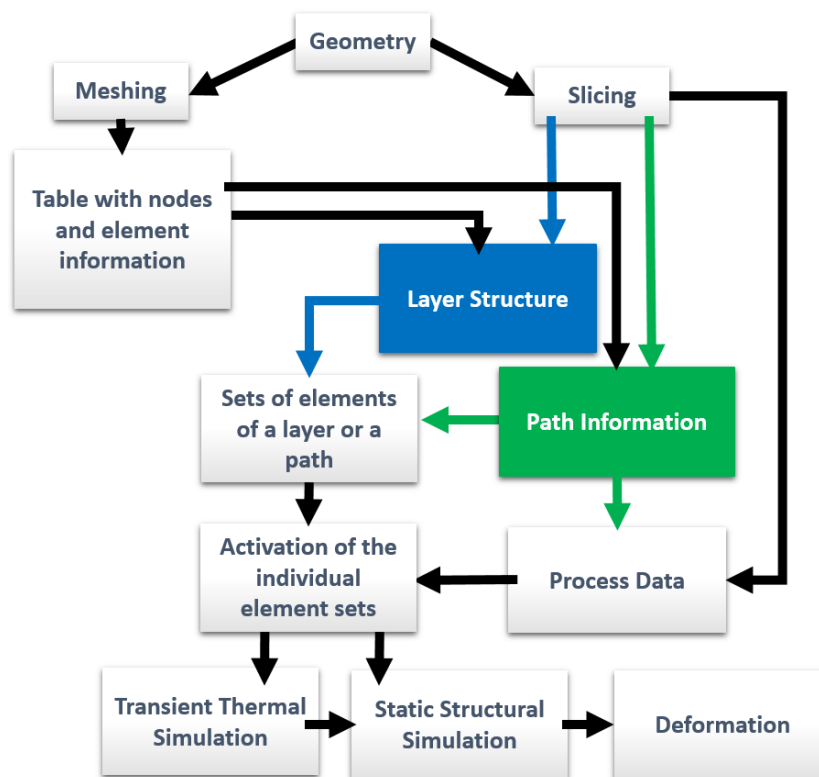


Fig. 5. Developed approach of the simulative mapping of the FLM process

The technology known as “birth/death” is used to model the process. This functionality is available in ANSYS with the scripting language Mechanical ANSYS Parametric Design Language (MAPDL). The challenge was to map the process, which was predefined by machine data and tool path, into the FEM program used by means of the “birth/death” technology and to express it with MAPDL commands. For an automated evaluation of the input data, as well as the generation of the settings and process data in the FEM software, an extension had to be programmed. The ANSYS Customization Toolkit (ACT) was used in ANSYS, which made it possible to develop functions that fully automatically prepare and execute the simulation.

3.2. INPUT DATA

In general, very detailed calculations can be carried out, as with the layer-by-layer and path-wise methods. For this, the component as well as the auxiliary structures and the build platform are required as separate geometries. Furthermore, the additional geometries generated by the slicer software, such as Brim or Skirt, are initially neglected and thus deleted for the FEM simulation. The geometry of the construction platform is necessary to realize the heat conduction from the component into the build platform and to map the heat capacity of the real construction platform. On the other hand, this is needed so that in the structure calculation, the structure of the component by a fixation as a boundary condition is not stiffened too much.

The Geometry was meshed with a body fitted cartesian mesh. The mesh size is automatically defined as a multiple of the layer thickness according to the machine data. This value can be modified to change the accuracy of the simulation.

For the modeling of the material PLA an orthotropic temperature-dependent elasticity and thermal expansion coefficient was assumed. For the implementation of the heat of fusion, an enthalpy had to be specified as a function of the temperature relative to 0 degree Celsius. All other material properties are assumed to be constant.

The prerequisite for the manufacturing process is that this ensures a continuous attachment of the part to the build platform to be manufactured. Therefore, a bounding condition between the part and the build platform is defined. Also, any defects during manufacture such as e.g. “Elephant foot”, “over extrusion”, “delamination” cannot be considered. Furthermore, it is assumed that the build space is perfectly completed and thus no forced convection can take place.

As was found in the literature and market research, so far only the layer wise approach is used. However, there are some restrictions. A limitation of the layer wise approach is that an entire layer is activated at a single time step and, for example, a multiple wall thickness cannot be represented. Another limitation of the stratified calculation is that individual layers are quasi homogenized by the assumption of a preferred direction. Exact effects of the alignment of individual path segments cannot yet be considered in this study.

With the method of path wise activation, thermal distributions caused by the trajectory can be well represented. In addition, layer-internal differences, such as, for example, the path orientation, can be represented, which have a significant influence on the behaviour of the part [32]. However, the path-wise method requires significantly more time steps for this by the individual activation of each path segment. This leads to an increased calculation time.

3.3. THERMAL SIMULATION

After processing the input data, all the information needed is now available to perform a transient thermal calculation. As described, the information was passed to the solver by means of MAPDL commands. These commands are written directly to the solver's input file using the automation developed.

The ambient temperature and temperature of the build platform are set to 20 degrees Celsius. All other settings e.g. extruder temperature, build time and layer thickness were taken from the G-code file, then processed and set by an automation scripted in Python. Thus, the initial temperature of the individual elements is taken from the extruder temperature information. In the specific case of the FLM process with the material PLA a temperature of 200 degrees Celsius is specified.

The conduction between the component and the building platform is realized via the contact condition and the thermal conductivity of the two bodies. For the definition of free convection, the heat transfer coefficient was needed to determine the energy exchange between the body and the environment in terms of time, free surface and temperature difference. For the application of air in a closed room, reference values from the literature [41] can be taken as a heat transfer coefficient h of $10 \text{ W}/(\text{m}^2\text{K})$.

In determining the time steps, on the one hand, the process and, on the other hand, the stability of the system had to be considered. In order to prevent overshoot or oscillation of the system, time steps had to be inserted at the beginning of the calculation without load application for the thermal calculation. As with the manufacturing of the samples, the part is cooled for a further 10 min without load after manufacturing.

In the path-wise approach, not all elements of a layer are activated at once, but several elements are activated in succession according to the G-code along the defined paths. The elements are activated with a predefined starting condition of 200 degrees Celsius. In addition, a convection is applied to all nodes lying on the surface. With this method, thermal distributions caused by the trajectory can be better represented. This requires individual sampling points. In the process, the toolpath trajectories are defined and grouped into individual segments as individual straight paths between two points. The absolute length of a segment is defined by the time required by the G-code. This can be adjusted to adjust the time resolution and accuracy of the process representation. The resulting increased number of sample points avoids element detection errors. However, in some cases, elements cannot be activated by a combination of unfavourably placed sample points and the path of the toolpath over the mesh. This exception is visualized in Fig. 6.

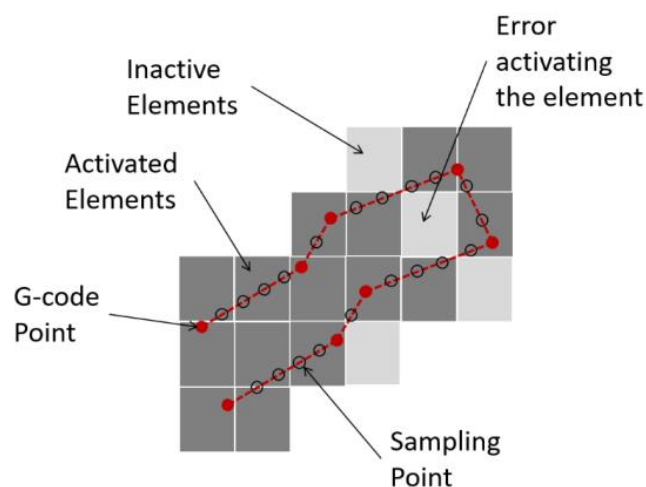


Fig. 6. Element detection error due to badly placed sample points

After defining the paths, programming is done for the calculation in a second MAPDL instruction. For the successive activation of the individual paths, all elements must first be deactivated before the first load step so that only the build platform can be reactivated in the following. The time step following shortly is used to clear the boundary condition of the temperature at the activated elements so that the elements can cool down freely.

This lasts until the next path specified by the G-code is activated. This process is repeated as long as paths are specified in the G-code and the entire component is constructed.

3.4. STRUCTURAL SIMULATION

With the temperature profile known from transient thermal simulation, the mechanical data can now be used to calculate the deformation (warping) caused by the process.

This mechanical distortion is caused by the thermal expansion coefficient when the local temperature deviates from the reference temperature. This means that the part requires the activation temperature and the build platform needs the ambient temperature as the reference temperature. This setting is automatically set by the programmed extension and checked before the calculation. As load variable in the structural mechanic calculation, the temperatures of the previous temperature field calculation are applied to the nodes of the model. This is done by reading in the result values of the temperature field calculation. For this purpose, the inhomogeneous temperature distribution is transferred to the corresponding time step on the mechanical model. It is important that the time steps of the mechanical calculation correspond to the time steps of the imported temperatures. In addition, the specifications of the mechanical boundary conditions are made.

In the case of path-wise calculation, the structural mechanical calculation must take analogous steps to the thermal calculation as far as possible. In this context, relationships between the time steps with the imported loads were also be taken into account. The time specified in the MAPDL command must be set equal to the time in the analysis settings. After these settings have been made by the developed program, the calculation can be started.

4. RESULTS OF THE THERMO-MECHANICAL FEM-SIMULATION

The results of the simulation performed are compared with the measurement results of FLM-printed specimen below. In the simulation, a method should be developed that can initially map the process of additive manufacturing with the provided input data and, without extensive investigation, it should be compared in terms of thermal distortion with the measurement results. The simulation or the calculation of the samples took place with the procedure described in Chapter 3.1 The sample geometry was meshed with an element size of 0.4 mm and the build platform with an element size of 5 mm. The number of time steps for the calculation varies depending on the specification from the G-code.

In the simulation with the configuration of the test series one to three with a printing speed of 45 mm/s, a single contour and a varying infill orientation of 0; 45; 90 degrees succeeded with the developed methodology of the path-wise activation to achieve a good mapping of the process. For example, in the calculation of the first series of tests, a maximum deformation in the upper level of 0.279 mm was calculated and by the evaluation of the levelness measurement (see Fig. 4) a deformation of 0.273 mm was determined. The accuracy of the simulation in comparison to the measurement is thus 2.35%. The scattering of the levelness measurement is only 0.06 mm.

When examining the measuring points in comparison to the simulation, good matches can be seen. For example, the deformation increases each time to the ends of the sample left and right (see Fig. 7 mark 1). In addition, a deformation around the hole can be seen in the simulation (see Fig. 7, mark 2). Remarkable is the strong bulge in the measurement result around the hole (see Fig. 7 mark 3), which, however, is due to a measurement error after visual inspection.

In addition to the simulation of the deformation, the course of the comparative stress (von Mises) was also analyzed. This is shown in Fig. 8 for this sample configuration. There, the increased residual stress after cooling in the lower region of the sample is clearly visible. In the case of failure of the component to adhere to the build platform, this effect produces the described “warping” (Section 3.4). Furthermore, it can be seen that these thermally induced residual stresses in the upper edges of the sample could be reduced by deformation. When calculating the test series with an increased wall thickness, only a minimal change in the results could be observed when using the layer wise method. Therefore, as described, the path wise method was used which provided more accurate results in the prediction of deformation in the FLM process.

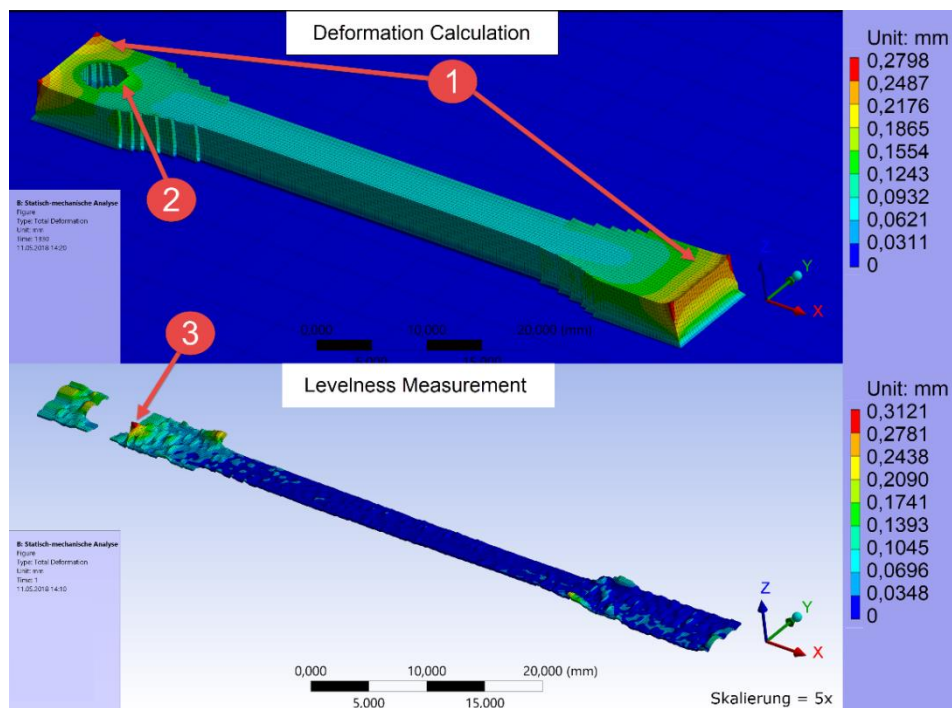


Fig. 7. Result of deformation calculation and levelness measurement of the first test series

REFERENCES

- [1] KRUTH J.P., LEU M.C., NAKAGAWA T., 1998, *Progress in Additive Manufacturing and Rapid Prototyping*, Annals of the CIRP, 47/2, 525–540.
- [2] MACDONALD E., WICKER R., 2016, *Multiprocess 3D printing for increasing component functionality*, Science, 353 (6307), <https://doi.org/10.1126/science.aaf2093>.
- [3] CHEN T., FRITZ S., SHEA K., 2015, *Design for mass customization using additive manufacture: case-study of a balloon-powered car*, Proceedings of the 20th International Conference on Engineering Design (ICED15), Milan, Italy.
- [4] THOMPSON M.K., MORONI G., VANEKER T., FADEL G., CAMPBELL R.I., GIBSON I., BERNARD A., SCHULZ J., GRAF P., AHUJA B., MARTINA F., 2016, *Design for Additive Manufacturing: Trends, opportunities, considerations, and constraints*, CIRP Annals – Manufacturing Technology, 65/2, 737–760.
- [5] SCHMIDT M., MERKLEIN M., BOURELL D., DIMITROV D., HAUSOTTE T., WEGENER K., OVERMEYER L., VOLLERTSEN F., LEVY G.N., 2017, *Laser based additive manufacturing in industry and academia*, CIRP Annals – Manufacturing Technology, 66/2, 561–583.
- [6] VEREIN DEUTSCHER INGENIEURE (VDI): VDI 3405 (*Additive Fertigungsverfahren. Grundlagen, Begriffe, Verfahrensbeschreibungen*).
- [7] GEBHARDT A., 2016, *Generative Fertigungsverfahren. Additive Manufacturing und 3D Drucken für Prototyping – Tooling – Produktion*, Carl Hanser Verlag, München.
- [8] ZHANG S., 2017, *Numerical evaluation of ABS parts fabricated by fused deposition modeling and vapor smoothing*, Advances in Science, Technology and Engineering Systems Journal, 2/6, 157–161 <https://doi.org/10.25046/aj020620>.
- [9] MORONI G., PETRO S., POLINI W., 2017, *Geometrical product specification and verification in additive manufacturing*, CIRP Annals – Manufacturing Technology, 66/1, 157–160.
- [10] DANTAN J.Y., HUANG Z., GOKA E., HOMRI L., ETIENNE A., BONNET N., RIVETTE M., 2017, *Geometrical variations management for additive manufactured product*, CIRP Annals – Manufacturing Technology, 66/1, 161–164.
- [11] ZHU Z., ANWER N., HUANG Q., MATHIEU L., 2018, *Machine learning in tolerancing for additive manufacturing*, CIRP Annals – Manufacturing Technology, 67/1, 157–160.
- [12] GORSKI F., WICHNIAREK R., KUCZKO W., ANDRZEJEWSKI J., 2015, *Experimental determination of critical orientation of ABS parts manufactured using fused deposition modelling technology*, Journal of Machine Engineering, 15/4, 121–132.
- [13] GORSKI F., WICHNIAREK R., KUCZKO W., 2014, *Influence of filling type on strength of parts manufactured by fused deposition modelling*, Journal of Machine Engineering, 14/3, 113–125.
- [14] ZÁH M., 2013, *Wirtschaftliche Fertigung mit Rapid-Technologien. Anwender-Leitfaden zur Auswahl geeigneter Verfahren*, Carl Hanser Verlag, München.
- [15] KUZNETSOV V.E., SOLONIN A.N., URZHUMTSEV O.D., SCHILLING R., TAVITOV A.G., 2018, *Strength of PLA components fabricated with fused deposition technology using a desktop 3D printer as a function of geometrical parameters of the process*, Polymers 2018, 10/313, <https://doi.org/10.3390/polym10030313>.
- [16] BENWOOD C., ANSTEY A., ANDRZEJEWSKI J., MISRA M., MOHANTY A.K., 2018, *Improving the Impact Strength and Heat Resistance of 3D Printed Models: Structure, Property, and Processing Correlations during Fused Deposition Modeling (FDM) of Poly (Lactic Acid)*, ACS Omega, 3/4, 4400–4411, <https://doi.org/10.1021/acsomega.8b00129>.
- [17] KELLER N., 2017, *Verzugsminimierung bei selektiven Laserschmelzverfahren durch Multi-Skalen-Simulation*, Dissertation, University of Bremen.
- [18] <https://www.ansys.com/de-de/products/structures/additive-manufacturing> *Additive Manufacturing Simulation*, Accessed 12 December 2018.
- [19] <https://www.autodesk.de/products/netfabb/overview> *Software für additive Fertigung und Konstruktion*, Accessed 12 December 2018.
- [20] <https://www.simufact.de/simufact-additive.html>, *Simufact Additive*, Accessed 12 December 2018.
- [21] <https://additive.works>, *Additive Manufacturing Software Solution of Tomorrow*, Accessed 12 December 2018.
- [22] <https://www.esi-group.com/de/software-loesungen/virtual-manufacturing/additive-fertigung>, *Mit Simulation metallische additive Fertigungsprozesse modellieren*, Accessed 12 December 2018.
- [23] <https://www.ge.com/additive>, *The Anything Factory*, Accessed 12 December 2018.
- [24] <https://alphastarcop.com/additive-manufacturing>, *Additive Manufacturing*, Accessed 12 December 2018.
- [25] <https://www.e-xstream.com/node/2856>, *Additive Manufacturing*, Accessed 12 December 2018.

- [26] TOFAIL S.A., KOUMOULOS E.P., BANDYOPADHYAY A., BOSE S., O'DONOGHUE L., CHARITIDIS C., 2017, *Additive manufacturing: Scientific and technological challenges, market uptake and opportunities*, *Materials today* 21/1, 22–37, <https://doi.org/10.1016/j.mattod.2017.07.001>.
- [27] FORD S., DESPEISSE M., 2016, *Additive manufacturing and sustainability: an exploratory study of the advantages and challenges*, *Journal of Cleaner Production*, 137, 1573–1587 <https://doi.org/10.1016/j.mattod.2017.07.001>.
- [28] YANG C., TIAN X., LI D., CAO Y., ZHAO F., SHI C., 2017, *Influence of Thermal Processing Conditions in 3D Printing on the Crystallinity and Mechanical Properties of PEEK Material*, *J. Mater. Process. Technol.* 248, 1–7, <https://doi.org/10.1016/j.jmatprotec.2017.04.027>.
- [29] Deutsches Institut für Normung e.V. (DIN): DIN EN ISO 527-2 (*Kunststoffe – Bestimmung der Zugeigenschaften*), Teil 2, 2012.
- [30] FARAH S., ANDERSON D.G., LANGER R., 2016, *Physical and mechanical properties of PLA, and their functions in widespread applications – A comprehensive review*, *Advanced Drug Delivery Reviews*, 107, 67–392, <https://doi.org/10.1016/j.addr.2016.06.012>.
- [31] MARIAN K., RIPPY M.K., BARON S., ROSENTHAL M., BRENT A., 2018, *Evaluation of absorbable PLA nasal implants in an ovine model: Biocompatibility of a PLA nasal implant*, *Laryngoscope Investigative Otolaryngology*, 3/3, 156–161, <https://doi.org/10.1002/lio2.166>.
- [32] MÖHRING H.-C., STEHLE T., BECKER D., EISSELER R., 2018, *Qualität von additive hergestellten PLA-Bauteilen*, *Werkstattstechnik online*, 108/6, 419–425.
- [33] SCHWARZL F., 2013, *Polymermechanik: Struktur und mechanisches Verhalten von Polymeren*, Springer-Verlag, Heidelberg.
- [34] MARTIENSSEN W., WARLIMONT H., 2005, *Handbook of Condensed Matter and Materials Data*, Springer-Verlag, Heidelberg.
- [35] LI Y., GAO S., DONG R., DING X., DUAN X., 2018, *Additive Manufacturing of PLA and CF/PLA Binding Layer Specimens via Fused Deposition Modeling*, *Journal of Materials Engineering and Performance*, 27/2, 492–500, <http://dx.doi.org/10.1007/s11665-017-3065-0>.
- [36] SHKUNDALOVA O., RIMKUS A., GRIBNIAK V., 2018, *Structural Application of 3D Printing Technologies: Mechanical Properties of Printed Polymeric Materials*, *Science – Future of Lithuania*, 10 <https://doi.org/10.3846/mla.2018.6250>.
- [37] CHACÓN J. M., CAMINERO M.A., GARCÍA-PLAZA E., NÚÑEZ P.J., 2017, *Additive manufacturing of PLA structures using fused deposition modelling: Effect of process parameters on mechanical properties and their optimal selection*, *Materials & Design*, 124, 143-157, <http://dx.doi.org/10.1016/j.matdes.2017.03.065>.
- [38] ULLU E., KORKMAZ E., YAY K., OZDOGANLAR O.B., KARA L.B., 2015, *Enhancing the structural performance of additively manufactured objects through build orientation optimization*, *J. Mech. Des.* 137/11, 111410, MD-15-1175, <https://doi.org/10.1115/1.4030998>.
- [39] LIU X., LI S., LIU Z., ZHENG X., CHEN X., WANG Z., 2015, *An investigation on distortion of PLA thin-plate part in the FDM process*, *Int. J. Adv. Manuf. Technol.*, 79, 1117–1126, <https://doi.org/10.1007/s00170-015-6893-9>.
- [40] VALERGA A.P., BATISTA M., SALGUERO J., GIROT F., 2018, *Influence of PLA Filament Conditions on Characteristics of FDM Parts*, *Materials* 11:1322, <https://doi.org/10.3390/ma11081322>.
- [41] Verein Deutscher Ingenieure e.V., 1994, *VDI-Wärmeatlas. Berechnungsblätter für den Wärmeübergang*, VDI-Verlag, Düsseldorf.